MGPB

Core Log and Cone Penetration Test Approach for Bearing Capacity Analysis of Quaternary Deposit and its Correlation to Facies Distribution in Southern Bali

Rudarsko-geološko-naftni zbornik
(The Mining-Geology-Petroleum Engineering Bulletin)
UDC: 551.3
DOI: 10.17794/rgn.2020.4.1

Professional paper

Nugroho Aji Satriyo[1]; Eko Soebowo[1]; Imam Achmad Sadisun[2]

[1]*Research Center for Geotechnology, Indonesian Institute of Sciences, Jl. Sangkurian, Kompleks LIPI – 40135, Bandung - Indonesia.*
[2]*Department of Geology, Bandung Institute of Technology (ITB), Jl. Ganesha No. 10 Lebak Siliwangi 40132, Bandung - Indonesia.*

Abstract

Area development deals with optimal land use and the reduction of the risk of geological disasters. The coastal area of South Bali is prone to land settlement hazards. In order to mitigate the risk, it is important to understand the depositional environment of the area related to its bearing capacity and geological hazard risks. The aim of this research is to understand the subsurface depositional environment and quantifying its bearing capacity. Quantitative modeling was carried out to obtain the sediment-bearing capacity of the Pendungan area in Bali, Indonesia. The methods used in this research were the observation of borehole cores, the identification of the cone penetration test (CPTu) curves pattern, the sediment index property test, the soil strength laboratory, and bearing capacity analysis. Based on lithologic association, the CPTu curve pattern, and grain size analysis, there are three facies developing in the study area with different bearing capacity values. Generally, beach ridge sand has a higher bearing capacity (N-SPT value of 8 – 52) for shallow foundation than fluvial clay. Meanwhile, floodplain facies has the lowest bearing capacity (N-SPT value of 2 – 20).

Keywords:
bearing capacity, sediment, CPTu, facies, southern Bali.

1. Introduction

The Southern Bali area includes Sanur, Serangan, and Pendungan, which are in a coastal zone, generally formed by the Holocene deposit of coastal plain. It's located in the Tanjung Benoa Basin and bordered by the Limestone South Formation in the southern part (**Hadiwidjojo et al., 1998**). This area is also included in a high earthquake vulnerability zone because it is located in ± 150 km south part of the active subduction zone. Shallow seismicity is centered in the plain of Bali caused by NW-SW or W-E fault activity (**McCaffrey & Nabalek, 1987**).

Area land capability and foundation design information are the most important factors which are required in area development. It is easily managed if accompanied by the foundation planning by adjusting the condition of the soil (**Burgart et al., 2015**). Furthermore, the aim of this study is to describe the subsurface condition in order to find the soil strength and whether or not it can resist load construction without the occurrence of shear failure and settlement state. Therefore, information on engineering geology is needed to support the plan. An engineering geological model such as vertical subsurface, engineering geology, and spatial condition can be the basic site or geological hazard impact study (**Kechebour, 2015**; **Rosye et al., 2009**; **URL, 2017**). It can also be used for identifying engineering geology problems and estimating material properties realistically (**Delgado et al., 2003**). Moreover, sediment bearing capacity and facies condition information of the development area are required in order to produce optimal construction.

Grain contact has a connection with bearing capacity because of physical characteristics which are contained by the facies. Sediment bearing capacity values that are obtained in every CPTu point are different due to geological factors influenced by the rock conditions, such as compactness, grain size distribution (as shown in **Figure 1**), grain contact, and water content (groundwater table). Furthermore, **Eslami et al. (2011)** and **Pariseau (2007)** explain that lithology physical characteristics have different height, size, shape, and sorting of the grain so it influences the internal friction angle and shear strength between the grain. Also, **Craig (2004)** and **Das (1997)** added that the bearing capacity is controlled by the factors such as grain size, permeability, and consolidation. It is explained that the value of bearing capacity in each facies will be different based on the lithology. Generally, bearing capacity is only used to recognize the sediment strength for surface loading pressure without any settlement occurring **(Das & Sivakugan, 2007)**. It is necessary to obtain further information related to the bearing capacity of shallow and deep foundation as a reference of physical development before the construction started.

Corresponding author: Nugroho Aji Satriyo
AjiSatriyo.Nugroho@gmail.com

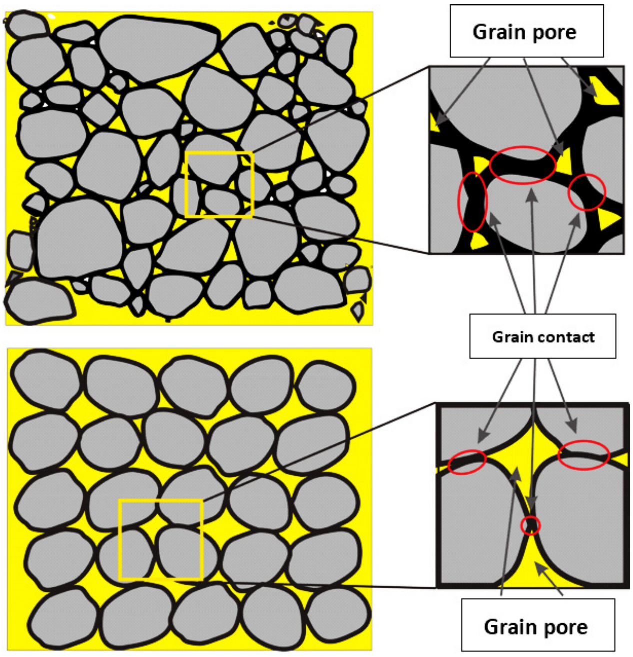

Figure 1: The connection between height, size, shape, and sorting of the grain related to grain contact and pore (modification from **Das & Sivakugan, 2007**)

Nevertheless, grain size and curve pattern analysis can show further information regarding the correlation between physical characteristics, facies development, and sediment bearing capacity. Based on research that has been conducted, the focus study on sediment bearing capacity can be related to the type of facies developed in a certain area.

1.1. Research location and geology

Most parts of Bali provinces are mountainous and hilly areas. Bali's island relief is west to east with elongated mountain chains. Among its mountainous areas, there are still active volcanoes, such as Agung Mountain (3.142 m) and Batur Mountain (1.717 m). Some other inactive volcanoes reach heights between 1,000 and 2,000 m. The central Bali mountain chain divides North Bali, which consists of narrow lower land from the foothill and mountain, from South Bali consisting of wide and plain lower land (see **Figure 2**).

Mainly analyzed from the elevation slope, Bali consists of a land of 0 – 2% to 15 – 40% elevation, the rest is land with an elevation of more than 40% (**URL 1, 2018**). The research area belongs to the southern physiography of Bali consisting of sedimentary and volcanic rocks. The characteristics of existing soils are more affected by volcanic weathering and alluvial deposits caused by an overflow of river transporting sediment. When flooding occurs, it will cause plated deposit structures in alluvial plains in low elevations.

Southern Bali coastal areas such as Sanur, Serangan, and Pendungan are areas formed by Holocene coastal plain deposits consisting of loose materials in the form of gravel, sand, silt and clay with a narrow to wide coastal plain (see **Figure 3**). The geology of this area is specified by dominant sandstone recurrence with fine to coarse grain size along with an intercalation of silt and clay. The depth of this Quaternary sediment reaches to a depth of around ± 20 m (**Soebowo et al., 2010**). The sediment of the coastal plain is a seismic zone path with high and active seismicity categorized into the 3rd, 4th, and 5th seismic zones (**URL 2, 2011**; **SNI 1726, 2012**). Therefore, the Bali coastal area is prone to geological hazards.

The geological setting of the Quaternary Bali Basin consists of alluvium deposits and early sediment, proven by shallow groundwater levels. The distribution of earthquake epicenters spread out to the front and back part of the subduction zone, while other parts are concentrated in the south arc of the Java, Bali and Nusa Tenggara islands. Seismic activity located in the surrounding oceanic trough is an earthquake produced by

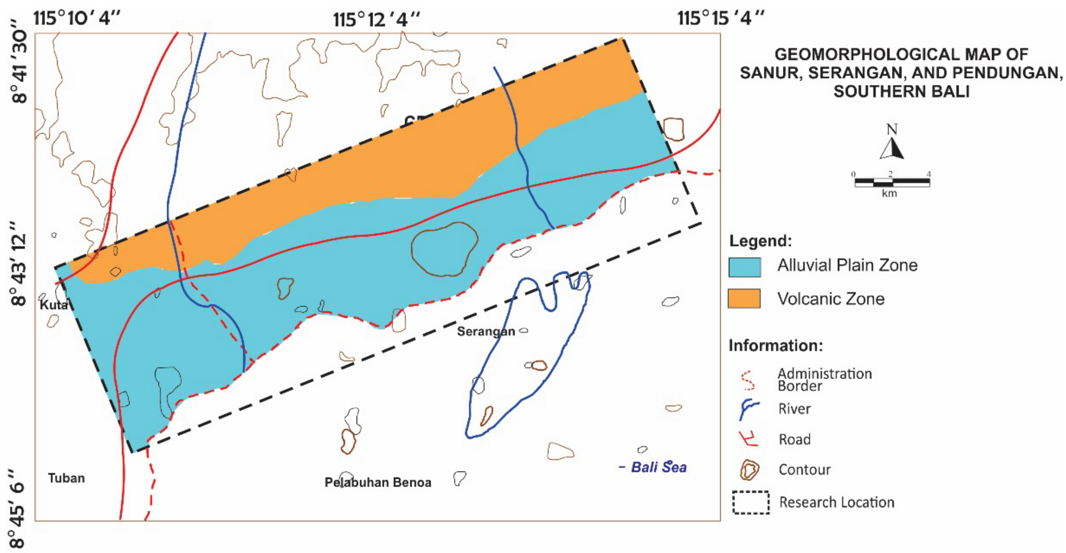

Figure 2: Geomorphological map of Southern Bali (Satriyo, 2017)

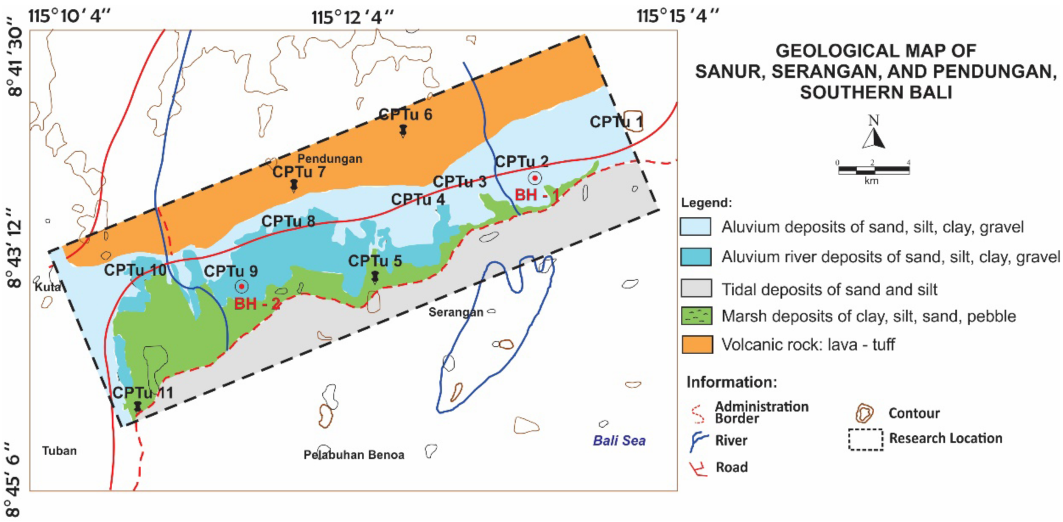

Figure 3: Geological map of Southern Bali (Satriyo, 2017)

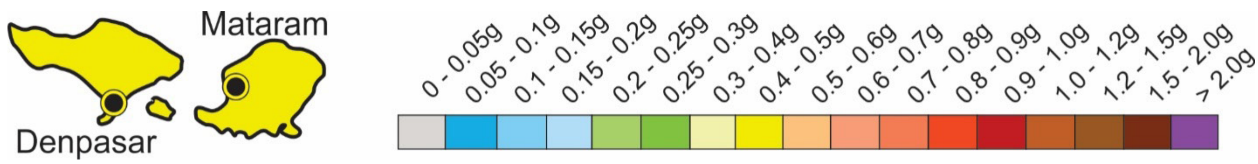

Figure 4: Hazard PGA 2% in 50 years (**Maps of Earthquake Indonesia, URL 3, 2017**)

intercontinental subduction. Shallow earthquake activity centered in the island of Bali is often caused by active faults which commonly shift from NW-SE or W-E (**McCaffrey & Nabalek, 1987**).

1.2. Previous Research

The South Bali coast is a part of Indonesia which has high earthquake hazard vulnerability because this area is located ± 100 – 150 km in the south part of an active subduction zone. In earthquake zonation maps, besides high earthquake hazard vulnerability, the South Bali coast is also located near active fault zones which cause shallow earthquakes, commonly in the SW-SE or W-E directions (**URL 2, 2011**).

Based on maps of Indonesian earthquake sources and hazards (**URL 3, 2017**), Bali is located in an area that has a peak bed acceleration of 0.4 – 0.5 g (see **Figure 4**). This means that the south coastal area has a lower vulnerability to earthquake hazards. The earthquake history of this site has recorded high earthquake occurrences such as in 1862: MMI VII, in 1890: MMI VII, in 1917: MMI VII, in 1938: MMI VII, in 1961: MMI VII in 1976: MMI VIII, in 1979: MMI VII - VIII, in 1985: 6.2 SR, in 1987: 5.7 SR, in 2004: 6.1 SR, 6.2 SR, 5.5 SR in southern Bali and the last time was on October 13, 2011 with 6.8 SR (**URL 4, 2017**).

A description of groundwater distribution in Pendungan – Sanur – Serangan, South Bali is generally reflected from river flow, habitat well and water drilling. Generally, the groundwater level is very shallow to shallow with a depth around 0.45 – 3.5 m and in other areas more than 3.5 m (**Seobowo et al., 2010**). This condition is influenced by the lithology factor which underlies the narrow South Bali plain on the beach part which consists of alluvial deposits, marsh deposits, and beach ridges. Quaternary sediment deposits in this area with narrow groundwater levels can lead to the possible occurrence of liquefaction in several locations (**Seobowo et al., 2010**).

2. Methodology

Geological area development is a concept associated with bearing capacity and geological aspects such as lithology, physical characteristics, and facies. In this research, several methods are used to prove if there is a correlation between all the aspects, such as 1) literature review, 2) engineering geology investigation, 3) data processing, 4) modeling and integrating data. Geological engineering investigation including 2 bore holes and 11 CPTu points (Cone penetration test with pore water measurement) has been done in a research study (see **Figure 3**). The locations of two bore holes are near the Pendungan area, where the first (BH-1) is in a private company's residence close to Ngurah Rai By Pass Street (with a maximum depth of 25 m) and the other (BH-2) is in the Department of Transportation of Denpasar City (with a maximum depth of 26 m) (see **Figure 3**). The laboratory analysis was carried out by the grain size method approach using a sieve shaker with a sample taken from a depth of 2 m and 10 m for clay and a depth of 1 m, 13 m, and 22 m for sand. At these depths, the samples are considered to represent lithological changes in the sediment layer of the research area.

Furthermore, N-SPT data taken from a drilling point that correlated to a depth and a suppression energy was used to interpret the engineering subsurface condition (**Roger, 2006**); for cohesive soil, cohesion and consistency estimation was implemented (see **Table 1**) and for non-cohesive soil, internal friction angle and the level of density estimation were used (see **Table 2**).

2.1. Data Analysis

2.1.1. Standard Penetration Test (SPT)

A SPT test is a test used to recognize in-situ sediment properties (**SNI 4135, 2008**). This test is done by hitting a standard tube to the bottom of the drill hole as deep as 45 cm by using a 63.5 kg hammer that falls freely from a height of 76 cm. The number of strokes required for penetration every 15 cm is recorded, but for the initial 15 cm, penetration is ignored because its sediment properties may be impaired at the time of drilling. **Meyerhof (1956)** and **Roger (2006)** stated that the amount of penetration in the last 30 cm was recorded as the N (N-value) which often correlated with sedimentary properties such as density, internal shear angle, and q_c value (see **Tables 1** and **2**).

Table 1: Consistency interpretation and undrained shear stress of cohesive soil from n-spt data (**Roger, 2006**)

Consistency	Cohesion (kPa)	N-SPT
Very soft	12	< 2
Soft	12 – 24	2 – 4
Firm	24 – 48	4 – 8
Stiff	48 – 96	8 – 15
Very stiff	96 – 192	15 – 30
Hard	192	> 30

Table 2: Level density interpretation and internal friction angle of non-cohesive soil from n-spt data (**Roger, 2006**)

Level of density	Relative Density (%)	Internal Friction Angle (°)	N-SPT
Very loose	< 0.2	< 30	< 4
Loose	0.2 – 0.4	30 – 35	4 – 10
Medium	0.4 – 0.6	35 – 40	10 – 30
Dense	0.6 – 0.8	40 – 45	30 – 50
Very dense	> 0.8	> 45	> 50

Rely on **Lunne et al. (1997)**, friction ratio (FR) value can be calculated as follows:

$$FR\ (\%) = fs\ /\ qc \times 100 \qquad (1)$$

Where:

fs – friction sleeve (MPa).

qc – conus resistance (MPa)

Conus pressure value (q_c) corrected to pore pressure (u), the result is a correction conus pressure value (q_t) as a:

$$qt = + (1 - a) \qquad (2)$$

Where:

qt – corrected conus resistance (MPa),

u – pore pressure (MPa),

a – ratio of conus area

Stratigraphy interpretation method from CPTu data using the SBT index curve (Equation 1 and 2) from **Lunne et al. (1997)** that has a good correlation to soil classification based on grain size **ASTM (2017)** and **Amorosi & Marchi (1999)**. The plotting process of conus resistance (q_t) to friction ratio is an expression of grain size, texture, and consistency, so it can be used to gain a subsurface stratigraphy profile (**Lunne et al., 1997**).

2.1.2. Cone Penetration Test with Pore Pressure (CPTu)

The CPTu test generates a subsurface stratification and engineering feature continuously. Furthermore, the primary application of the CPTu is to measure soil resistance, providing a classification of the soil texture with depth for geotechnical purposes (**Begemann, 1965**). The obtained soil response parameter is a profile of conus resistance (q_c), friction sleeve (f_s), pore pressure (u_2). The conus resistance value (q_c) indicates soil density and consistency, while the friction sleeve (f_s) is represented in the friction ratio (FR) parameter which is a transformation of grain size and texture (see **Figure 5**).

Engineering geological analysis was performed in a way to compile subsurface stratigraphy and engineering properties based on lithology, CPTu and N-SPT value interpretation, relative density parameters and laboratory results. Then, the correlation process is done between the subsurface section which describes the engineering properties and spatial interpolation, depth variation and layer thickness so a horizontal and spatial description of engineering properties can be obtained. The correlation and interpolation process also describes the bearing capacity zone of the land capability of cohesive and non-cohesive soil so that it points out which areas have a soil capacity that is suitable for construction.

The N-Value is dominated by the amount of energy resulted by the SPT in the bore hole (**Kovacs et al., 1981**) and (**Schertmann, 1978**). **Douglas & Olsen (1981)** explain that the type of hammer will result in a significant q_c /N ratio rather than soil density. Furthermore, a study conducted by **Kovacs et al. (1981)** has shown that the q_c /N relies on the fine content of sandy soil. From the studies, major factors that can influence the q_c/N ratio are permeability and compressibility modification of the sand. **Sanglerat (1972)** reviewed and presented a number of studies implemented in several countries. A variety of these studies have assigned a constant ratio of

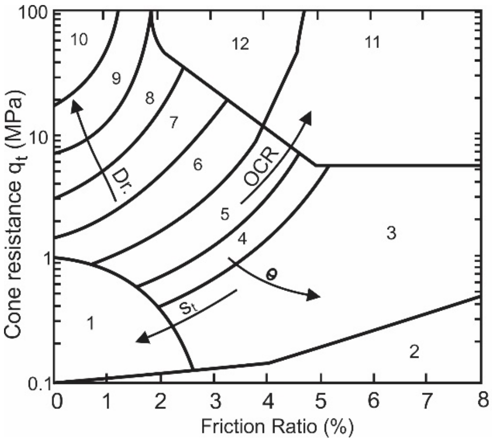

Zone	Soil Behaviour Type
1	Sensitive fine grain
2	Organic material
3	Clay
4	Silty clay to Clay
5	Clayey silt to silty clay
6	Sandy silt to clayey silt
7	Silty sand to sandy silt
8	Sand to silty sand
9	Sand
10	Gravelly sand to sand
11	Very stiff fine grained
12	Sand to clayey sand

Figure 5: Soil type diagram modification from **Lunne et al. (1997)**

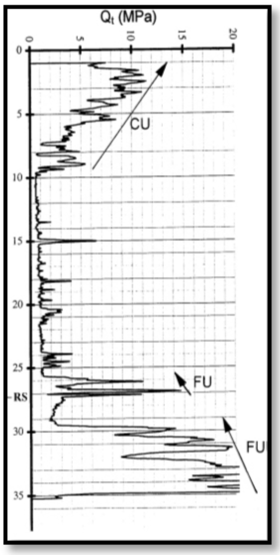

CYLINDRICAL	*FUNNEL SHAPE*	*BELL SHAPE*	*SYMMETRICAL*	*CRESSENTIK*
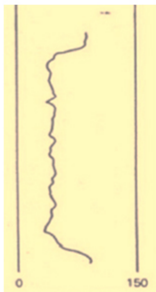			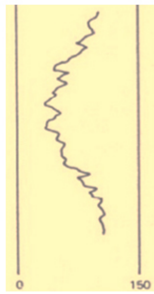	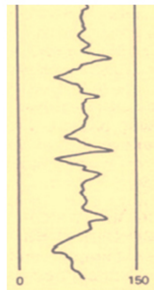
Braided fluvial channel	Distributary mouth bar, barrier island	Fluvial point bar Tidal poin bar some transgressive shelf sand	Sandy offshore bar, some transgressive shelf sand	Fluvial flood plain

Figure 6: A comparison between CPTu (left) and gamma ray log (right)
(**Amorosi & Marchi, 1999**; **Valverde-Palacios et al., 2014**)

q_c /N for each soil type; for instance, sandy soils have mostly q_c /N ratios larger than 4, while clays have ratios less than 4 (**Jarushi et al., 2015**). Furthermore, these studies have drawn important conclusions that an increase in soil compactness and relative density would decrease the q_c /N ratio (**Jarushi et al., 2015**).

The determination of the developed depositional environment in the study area used the comparison between gamma ray, borehole sample and CPTu. A borehole sample is used for cross-checking the grain size distribution and description. In its description, gamma-ray logs are one of the logs in the petroleum industry commonly used for lithologic interpretation, and the principle is the evaluation of the shale content (V-shale) or fine fraction and records grain size changes of a sediment through a certain curve pattern. CPTu is a commonly used geotechnical tool for determining the geotechnical sediment properties and describes the sediment stratigraphy. The CPTu principle is to calculate the end/strength and adhesive resistance which will be used for lithologic interpretation through fine fraction content, in addition, CPTu also records large grain changes through certain curve patterns. Looking at the information, both tools can be compared to the interpretation of geological lithology and facies (see **Figure 6**) (**Slatt et al., 1992**). Several studies regarding the use of CPTu for bearing capacity in some purposes have been done. For example, predicting the bearing capacity of a bored pile (**Iyad et al., 2015**) and a piled foundation (**Nicolay et al., 2017**).

This method consists of pressing a pile to examine the penetration or shear resistance. The pile can either be a round pole or a closed round pipe with a conical end and/or a soil sampling tube, so it can estimate the physical properties of a layer and the locations with variations of resistance at the time of the erection of the tool (**Lunne et al., 1997**). This method serves for exploration and in-situ testing.

One way to calculate the shallow strength of the shallow foundation commonly used in Indonesia by the field testing method is the cone penetration test (CPTu). The shallow bearing capacity of the foundation is found by using simple conversion formulas. Below, some formulas of shallow ground capacity based on CPTu data will be shown. The measurement of allowed and ultimate bearing capacity (q_{all} and q_{ult}) of cohesive and non-cohesive soil can be obtained from:

Sandy soil (non-cohesive):

- **Meyerhof (1956)**

$$q_{all} = \frac{q_c}{30} \quad (3)$$

- **Sanglerat (1972)**

$$q_{all} = (B.q_c / 40)x(1 + B / D_f) \quad (4)$$

- **Schmertmann (1978)**

$$q_{ult} = \gamma D_f N_q + 0,5\gamma B N_\gamma \quad (5)$$

Clayey soil (cohesive):

- **Schmertmann (1978)**

lane foundation

$$q_{ult} = 2 + 0,28 q_c \quad (6)$$

square foundation

$$q_{ult} = 5 + 0,34 q_c \quad (7)$$

Sandy or clayey soil:

- **Meyerhof (1956)**

$$q_{ult} = q_c(\frac{B}{12,2})(1 + \frac{D_f}{B}) \quad (8)$$

$$q_{all} = \frac{P_{ult}}{3} + \frac{F_{ult}}{5} = \frac{A(q_c)}{3} + \frac{O(JHP)}{5} \quad (9)$$

where:

q_{all} = allowed bearing capacity (q_{ult}/3, score 3 is a safety factor)
q_{ult} = ultimate bearing capacity
q_c = average conus penetration arithmetic q_c from base foundation to 1.5B under foundation
P_{ult} = conus tip resistance
F_{ult} = conus sleeve resistance
B = foundation width (assumed of 1 meter)
D_f = foundation depth
γ = effective soil density around foundation (1000 kg/m^3)
N_q and N_γ = non-dimensional bearing capacity factor

In the formulas above, the allowed (q_{all}) and ultimate (q_{ult}) bearing capacity score for non-cohesive soil conditions can be calculated using the parameters approach of conus resistance (q_c), foundation width (B), and foundation depth (D_f) (Equations 3, 4, and 5) (**Meyerhof, 1956**; **Sanglerat, 1972**; **Schmertmann, 1978**). However, for cohesive soil such as clayey and silty sand, **Schmertmann (1978)** explain that for ultimate bearing capacity (q_{ult}) should add the type of foundation, for example lane or square foundation (see Equations 6 and 7). Furthermore, **Meyerhof (1956)** added, the calculation of ultimate bearing capacity (q_{ult}) in a mixture of soil between sandy and clayey soil should add up several parameters such as conus tip resistance (P_{ult}), conus sleeve resistance (F_{ult}), and conus diameter ($A(q_c)$) (see Equations 8 and 9).

3. Results and discussion

3.1. Develop Facies

Qualitative interpretation was performed on three drilling cores and three CPTu curves residing in the research area (see **Figure 7**) to determine whether or not they had developed facies, which would then become the object of the study. The four CPTus' (CPTu 01, CPTu 03, CPTu 4, and CPTu 10) were paired with two boreholes (BH 01 - BH 02) to assist the facies analysis based on observing the CPTu curve pattern. The CPTu and bores were carried out to a depth of less than 30 m. From the observation of lithologic association with the observation of the CPTu curve pattern, there were three facies that developed in the research area. Several factors such as thickness, sediment type, and the physical properties of sediments also distinguish the three facies.

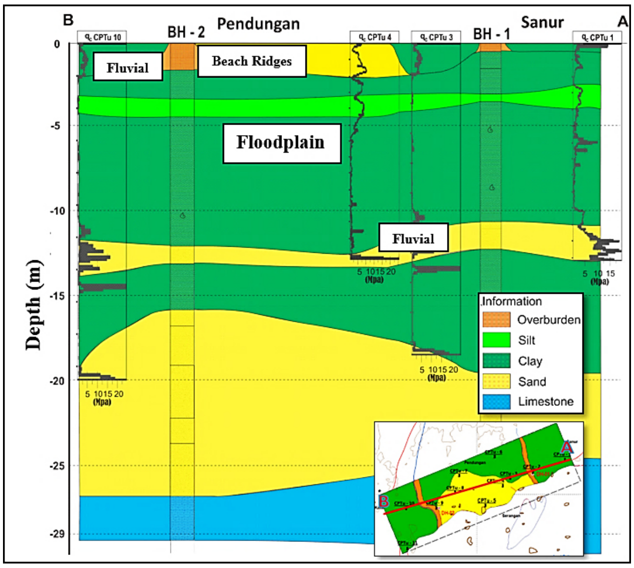

Figure 7: The subsurface section as the correlation result of four CPTus' (CPTu 01, CPTu 03, CPTu 4, and CPTu 10) are paired with two boreholes (BH 01 - BH 02)

3.2. Facies of Flood Plains

Based on the lithology characteristics, the floodplain clay facies are dominantly composed of clay and silt. The clay is colored dark-gray-green, and is soft, with a mixture of shells, while the silt is gray in color with a slightly soft to moderate density, with a thickness of 1.5 - 10 m, and both are located at a depth of 0.5 - 10.5 m (BH-01). In general, these facies occupy 50% of the re-

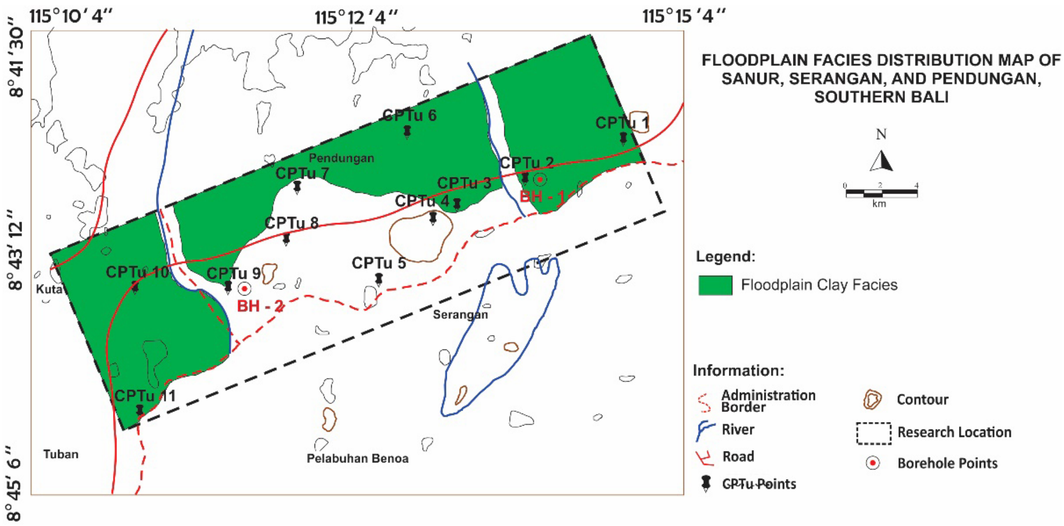

Figure 8: Lateral dispersal Maps of flood plain clay facies (Satriyo, 2017)

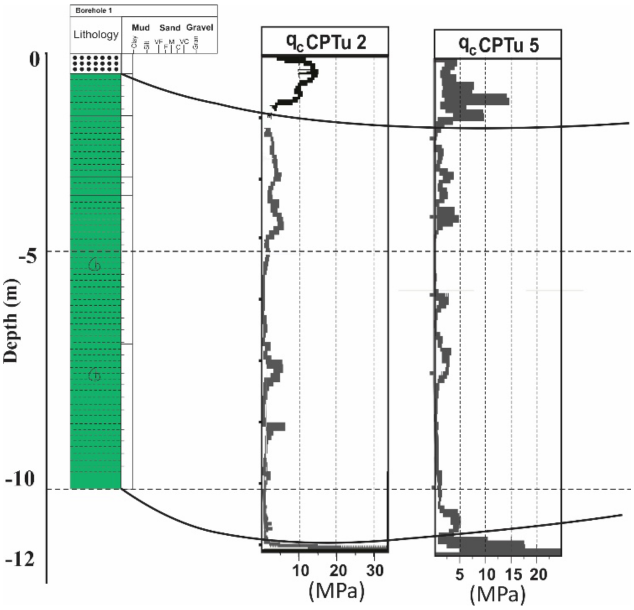

Figure 9: A comparison between BH-01 with CPTu 2 and CPTu 5 for determination of the flood plain clay facies

search area, dominantly in the north, east, and west of the study area (see **Figure 8**).

Based on the observation of the CPTu curve, the facies are characterized by a crescentic curve (**Walker and James, 1992**) with a value of 0.5 – 5 MPa (see **Figure 9**). The floodplain clay facies have varying N-SPT, ranging from 2 – 20 (very soft to slightly dense) as shown in **Figure 9**.

3.3. Clay and Sand Fluvial Facies

Based on its lithologic features, the facies are composed of clay and sand. The clay is dark gray to brown, of medium density, contains gravel, and is located at a depth of 0 – 1.5 m (see **Figure 10**). Meanwhile, the sand is white-brown to gray white, medium to coarse sand, poorly sorted, rounded to sub rounded, very dense, does not contain shells of sea fauna, with a thickness of 1 – 2 m, and is located at a depth of 10.5 – 12 m (see **Figure 11**). In general, this facies occupies 10% of the study area (see **Figure 12**).

Based on the observation of the CPTu curve pattern, the facies is characterized by an uneven, symmetrical, and fining upward (FU) (**Walker and James, 1992**) with a q_c value of 6 - 17 MPa (see **Figure 10** and **Figure 11**). Physically, clay and sand fluvial facies have varia-

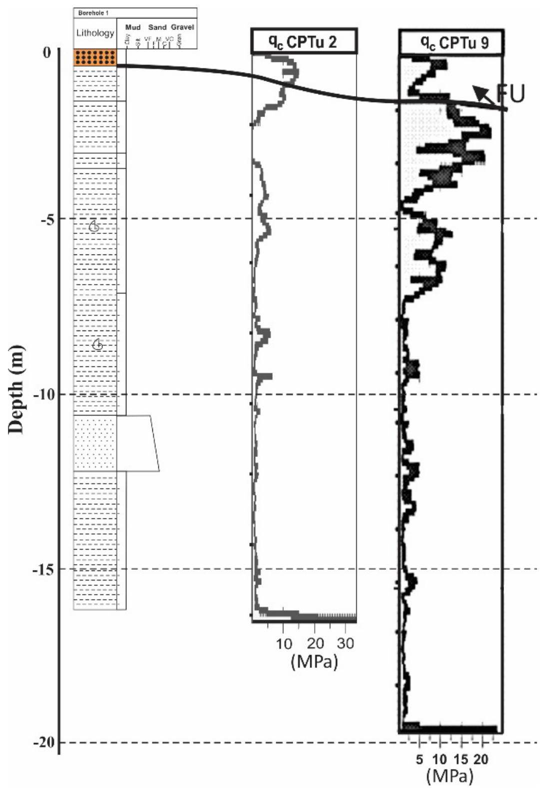

Figure 10: A comparison between BH-01 with CPTu 2 and CPTu 9 for the determination of clay fluvial facies.

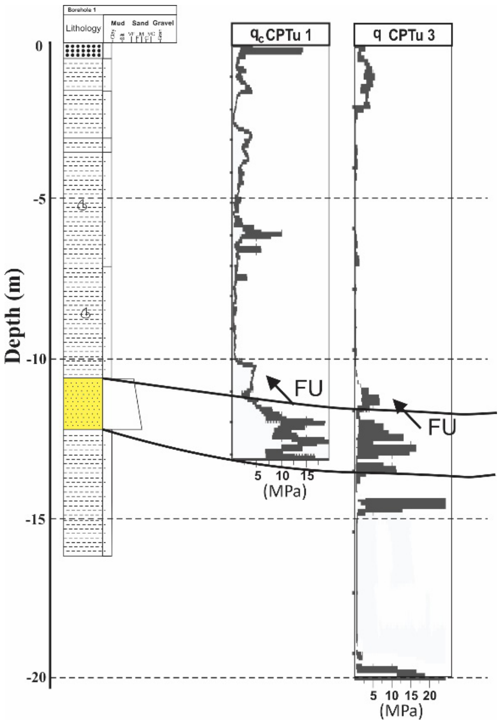

Figure 11: A comparison between BH-01 with CPTu 1 and CPTu 3 for the determination of sand fluvial facies.

ble N-SPT, ranging from 24 to 68 (medium dense to very dense).

3.4. Beach Ridge Sand Facies

Beach ridge sand facies are generally composed by the lithology of fine to coarse sand, feculent white, well sorted, sub angular to sub rounded with the degree of density from very loose to medium dense. This facies has a thickness of 2 m (see **Figure 13**) and it's located at a depth of 0 – 2 m (BH-02). Beach ridge sand facies generally occupy 40% covering the center of the study area (see **Figure 14**).

The typical pattern of the CPTu curve that characterizes the beach ridge sand facies is coarsening upward (CU) (**Walker and James, 1992**) (see **Figure 13**). This facies has a range of q_c values between 2 - 13 MPa (see **Figure 13**). The type of developed sediment and N-SPT possessed by beach ridge sand is also more varied than fluvial sand facies.

3.5. Shallow and Deep Bearing Capacity Score of Research Location

Scoring analysis has been done using data regarding grain size, depth, sediment type, CPTu, and N-SPT. This analysis uses 1 meter length (L) and width (B) of foundation with a depth (D_f) of also 1 meter (**SNI 1727, 2013**). For the measurement of deep bearing capacity, 2 types of foundations were used (**SNI 1727, 2013**), which are:

1. a circle-shaped foundation with a diameter (D) of 1 meter, a cross-sectional area (Ap) of 0.785 m^2, and
2. a square-shaped foundation with a length side of 1 meter.

The results of calculating the bearing capacity score of shallow sediment foundations in the research location resulted in a fairly variable range of values (see **Table 3**). The value is influenced by physical characteristics and lithology that developed in the study area.

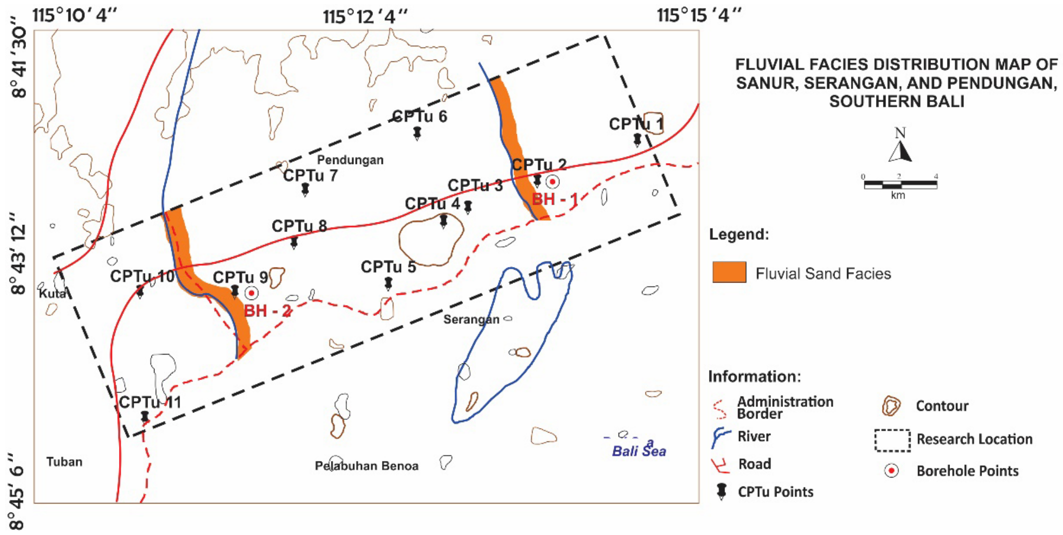

Figure 12: Lateral dispersal maps of sand fluvial facies (Satriyo, 2017)

From the values of bearing capacity of shallow foundation sediments obtained from CPTu, further determination of the minimum and maximum value of the total value of CPTu was achieved by using statistical analysis. After the value of shallow foundation bearing capacity is obtained for each CPTu, the next step is to group facies based on the CPTu curve pattern and the q_c value. The aim is to discover which areas have the lowest to the highest bearing capacity and their relationship with the distribution of facies.

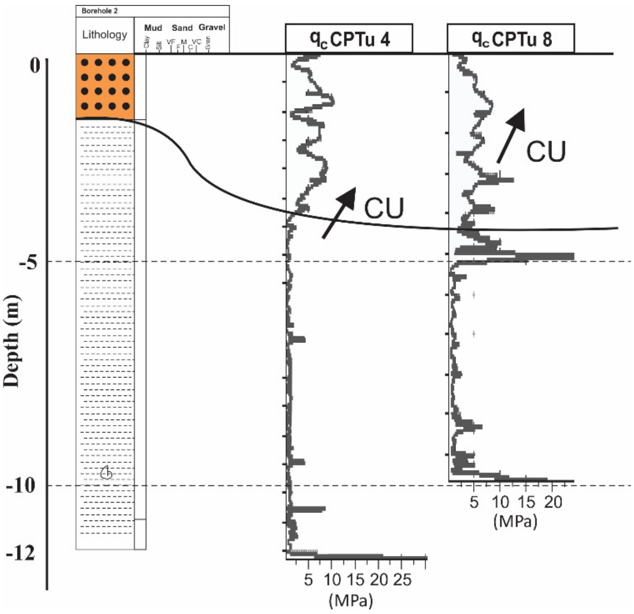

Figure 13: A comparison between BH-02 with CPTu 4 and CPTu 8 for the determination of beach ridge facies

The analysis calculation result was obtained by grouping the value of each CPTu and subsequently classifying the soil classification based on the British Standard (BS) number 8004 (**BS 8004, 2015**) so that the type of land classification developed at each point on CPTu in the research area can be known (see **Table 3**). From these results, the classification of soils at each of these CPTu points indicates that the type of sediments developing in the study area is dominated by dense sand and soft clays, but does not indicate if the lithology is only clay, silt, or sand because a mixture of mud and gravel was found in the area, as shown in the physical description.

The value of sediment deep foundation bearing capacity in the research area is done by calculating N-SPT in log drill BH-01 and BH-02 (see **Table 4**) by using a circle pile with a diameter of 1 m and a square shape with a side length of 1 m (**SNI 1727, 2013**).

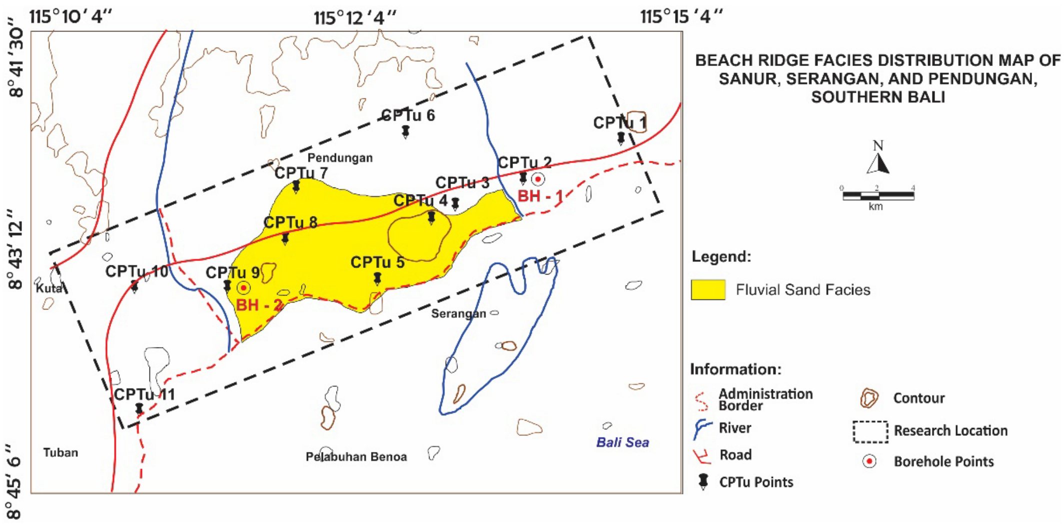

Figure 14: Lateral dispersal maps of beach ridges facies (Satriyo, 2017)

Table 3: Bearing capacity score of shallow foundation of each CPTu points, sediment bearing capacity score, and soil consistency (**Bowles, 1995**; **BS 8004, 2015**)

CPTU	q_c score (MPa)	Ultimate bearing capacity (kN/m²)	Allowable bearing capaity (kN/m²)	Soil classification BS 8004 (2015)
CPTU 1	3	369.12	123.04	Firm clay
CPTU 2	4	568.54	189.51	Stiff clay
CPTU 3	1	275.41	91.8	Firm clay
CPTU 4	8	1591.25	530.42	Medium dense sand
CPTU 5	4	2163.49	721.16	Dense sand
CPTU 6	4	295.81	98.6	Firm clay
CPTU 7	9	1632.05	544.02	Medium dense sand
CPTU 8	7	1785.06	59502	Medium dense sand
CPTU 9	17	693.62	231.21	Medium dense sand
CPTU 10	1	336.61	112.2	Firm clay
CPTU 11	5	408.01	136.04	Firm clay

Table 4: bearing capacity score of deep foundation based on n-spt in log drill bh-01 and bh-02 for a circle and a square section.

Depth (m)	Circle section				Square section		
	Q Ult (kN/m²)	Q All (kN/m²)	Q All (ton)		Q Ult (kN/m²)	Q All (kN/m²)	Q All (ton)
5	554.21	154.8	15.79	BH-01	992	254.4	25.96
10	1,231.72	334.26	34.11		2,298.13	571.63	58.33
10.5	2,927.32	868.06	88.58		4,758.13	1,311.62	133.83
12.5	1,719.46	369.01	37.65		4,140.8	860.16	87.77
15	1,803.19	385.76	39.36		4,354.13	902.83	92.13
20	4,251.35	1,132.87	115.59		8,131.46	1,986.29	202.68
24.5	5,852.75	1,484.55	151,48		27,171.4	8,100.96	826.62

Depth (m)	Circle section				Square section		
	Q Ult (kN/m²)	Q All (kN/m²)	Q All (ton)		Q Ult (kN/m²)	Q All (kN/m²)	Q All (ton)
5	366.33	98.38	10.04	BH-02	693.33	170.67	17.41
10	999.46	256.41	26.16		2,006.4	473.28	48.29
15	3,215.36	844.03	86.13		6,272	1,510.4	154.12
20	3,311.65	838.17	85.53		6,757.33	1,575.47	160.76
24.5	5,714.8	1,406.7	143.54		12.04	2.74	280

4. Discussions

4.1. Floodplain Clay Facies, Physical Properties, and The Bearing Capacity Score

Floodplain clay facies are generally composed of clay and silt. Physically, this facies has an N-SPT ranging from 2 - 20 (soft to slightly dense). Based on the calculation analysis of the bearing capacity, this facies has the highest shallow foundation bearing capacity score of 136.04 kN/m², and deep foundation bearing capacity scores of 868.06 kN/m² (circle foundation) and 1,311.62 kN/m² (square foundation) (see **Table 4**). This condition shows compatibility with the values generated from CPTu data (see **Tables 5** and **6**).

4.2. Fluvial Sand Facies, Physical Properties, and the Bearing Capacity Score

Based on its lithologic features, the fluvial sand facies are generally composed of medium sand to coarse sand with an N-SPT ranging from 24 - 68 (dense to very hard). This facies has the highest shallow bearing capacity score of 231.21 kN/m², and the deep bearing capacity values of the foundation in this facies are 369.01 kN/m² (circle foundation) and 860.16 kN/m² (square foundation) (see **Table 4**). This illustrates that this facies has a bearing capacity higher than the bearing capacity found in the floodplain facies. The density level of the facies of a floodplain is smaller than the density in fluvial facies

Table 5: The shallow foundation bearing capacity score based on CPTu in floodplain facies at a depth of 3 meters

CPTu	q_c Score (MPa)	Ultimate bearing capacity (kN/m²)	Allowable bearing capacity (kN/m²)	Soil classification BS 8004 (2015)
CPTu 1	3	369.12	123.04	Firm clay
CPTu 3	1	275.41	91.8	Firm clay
CPTu 6	4	295.81	98.6	Firm clay
CPTu 10	1	336.61	112.2	Firm clay
CPTu 11	5	408.01	136.04	Firm clay

Table 6: The deep foundation bearing capacity score based on CPTu in floodplain facies

Depth (m)	CPTu 1 (kN/m²)	CPTu 3 (kN/m²)	CPTu 6 (kN/m²)	CPTu 10 (kN/m²)	CPTu 11 (kN/m²)
5	189.61	125.69	227.53	104.33	280.1
10	399.80	306.99	249.99	173.46	501.3
15		302.31	2424.25	932.58	
20		1521.53		821.82	

Table 7: The shallow foundation bearing capacity score based on CPTu in fluvial facies at a depth of 3 meters.

CPTu	q_c (MPa)	Ultimate bearing capacity (kN/m²)	Allowable bearing capacity (kN/m²)	Soil classification BS 8004 (2015)
CPTu 2	4	568.54	189.51	Stiff clay
CPTu 9	17	693.62	231.21	Medium dense sand

Table 8: The deep foundation bearing capacity score based on CPTu in fluvial facies.

Depth (m)	CPTu 2 (kN/m²)	CPTu 9 (kN/m²)
5	172.47	192.73
10	348.42	296.18
15	394.91	835.48
20		849.67
25		1824.76

because it has a low N-SPT score. The mean score of q_c and N-SPT of these facies are 11.5 and 42, thus showing that the physical and engineering characteristics possessed by this fluvial sand reflect its good sediment bearing capacity when used as the foundation at a depth of 10.5 - 12.5 m, which is in correlation with the bearing capacity value found in CPTu data (see **Tables 7** and **8**).

4.3. Beach Ridge Sand Facies, Physical Properties, and The Bearing Capacity Score

Based on its lithologic features, the beach ridge sand facies are generally composed of medium to coarse sand. This facies has N-SPT values ranging from 8 - 52 (loose to very hard). The highest shallow bearing capacity for this facies is 721.16 kN/m² and the deep bearing capacity scores of the foundation are 98.39 kN/m² (circle foundation) and 170.67 kN/m² (square foundation) (see **Table 4**). This state also has correlation with CPTu measurement, as seen in **Tables 9** and **10**.

There are 2 divisions of territory including shallow and deep bearing capacity. Generally, the area with good shallow bearing capacity is the beach ridge, especially at depths less than 4 m. However, areas that have good foundation carrying capacity values, particularly those with a recommended depth of more than 10 m, are areas that can be found throughout the entire research site, as seen in **Figure 15**.

Table 9: the shallow foundation bearing capacity score based on CPTu in beach ridge facies at a depth of 3 meters

CPTu	q_c (MPa)	Ultimate bearing capacity (kN/m²)	Allowable bearing capacity (kN/m²)	Soil classification BS 8004 (2015)
CPTu 4	8	1591.25	530.42	Medium dense sand
CPTu 5	4	2163.49	721.16	Dense sand
CPTu 7	9	1632.05	544.02	Medium dense sand
CPTu 8	7	1785.06	595.02	Medium dense sand

Table 10: the deep foundation bearing capacity score based on CPTu in beach ridge facies

Depth (m)	CPTu 4 (kN/m²)	CPTu 5 (kN/m²)	CPTu 7 (kN/m²)	CPTu 8 (kN/m²)
5	275.17	144.28	1516.19	219.88
10	328.02	368.29	3116.48	294.33
15		307.95		

5. Conclusions

Relying on data analysis from two boreholes and CPTu identification, there are 3 developed facies in the research area, which are floodplain clay facies, fluvial clay and sand facies, and beach ridge sand facies. Vertical facies changes can be identified from 2 existing boreholes, i.e.:

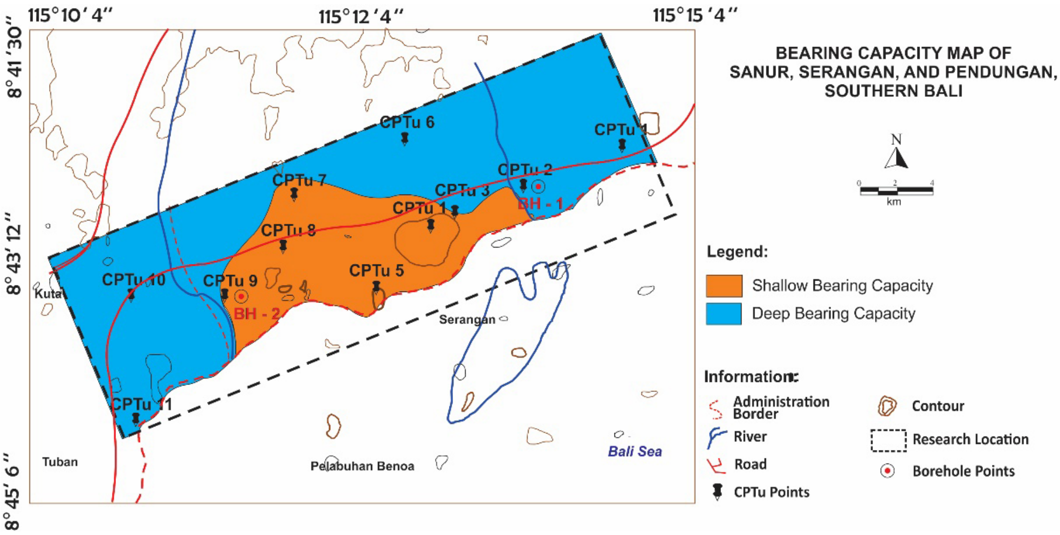

Figure 15: Bearing capacity map of South Bali, Bali Island (Satriyo, 2017)

- In BH-01, the fluvial clay facies are at a depth of 0 – 0.5 m, from a depth of 0.5 – 10.5 m of the facies transformed into a clay floodplain facies.
- At BH-02, the fluvial sand facies are at a depth of 11.5 – 12.5 m, from a depth of 12 - 15.25 m the facies turn into facies of floodplain clay.

Based upon physical characteristics and bearing capacity analysis, each facies has different values; the floodplain facies has the lowest value and the beach ridge facies has the highest shallow foundation bearing capacity value. Nevertheless, in cases of deep foundation bearing capacity, floodplain facies have the highest bearing capacity value since they have the deepest depth and the beach ridge has the lowest value because it has the shallowest surface. All this proves that bearing capacity of the facies is controlled by depth, natural compaction, grain size distribution, and the lithology of each sediment layer. Based on the value of bearing capacity, this research recommends the use of square foundations, which have a higher value than circle foundations. Moreover, this circular foundation has a wider base area in comparison to a square foundation in the same width of 1 meter, which is something to keep in mind when working in residential areas. Besides, in terms of geotechnics, a square foundation can support development because it can be used in the shallow layer with a maximum of 3 meters, thus, it can be more efficient in the use of development funds. However, if the construction is intended to build a two-story building or more, it is better to add to the depth of fluvial sand facies, which is at a depth of 11.5 meters.

Acknowledgement

The authors would like to thank to Dr. Haryadi Permana as the director of Research Centre for Geotechnology, Indonesian Institute of Sciences (LIPI) for the opportunity to take part in the research of Bali's quaternary sediment and for supporting all activities and administration. The publication of this research is supported by the funding scheme of the Deputy of Earth Sciences of the Indonesian Institute of Sciences (LIPI).

6. References

ASTM D2487-17 (2017): Standard Practice for Classification of Soils for Engineering Purposes (Unified Soil Classification System), ASTM International, West Conshohocken, PA, link: http://www.astm.org/cgi-bin/resolver.cgi?D2487

Amorosi, A. and Marchi, N. (1999): High resolution sequence stratigraphy from piezocone test: an example from Late Quaternary deposits of the southeastern Po Plain, Sedimentary Geology, 128, 67 – 81.

Begemann, H.K.S.Ph. (1965): The Friction Jacket Cone as an Aid in Determining The Soil Profile. Proceeding 6th International Conference on Soil Mechanic Foundation Engineering, 1, 17 – 20 p.

Bowles, J.E. (1995): Foundation analysis and design, McGraw-Hill Science, New York, 1169 p.

BS 8004 (2015): Code of Practice for Foundation. British Standard Institution, London, 112 p.

Burghart, W., Morel, J.L., and Zhang, G.L. (2015): Development of the soil research about urban, industrial, traffic, mining, and military areas (SUITMA). Soil Science and Plant Nutrition, 61, 3 – 21.

Craig, R.F. (2004): Craig's Soil Mechanics, (7 eds.). Spon Press: Taylor and Francis Group, London, 443 p.

Das, B.M. (1997): Advanced Soil Mechanics. (2nd edition.). Taylor and Francis Group, London and New York, California State University, Sacramento, 712 p.

Das, B.M. and Sivakugan, N. (2007): Settlements of shallow foundations on granular soil: an overview. International Journal of Geotechnical Engineering, 1 (1), 19 – 29 p.

Delgado, J., Alfaro, P., Andreu, J.M., Cuenca, A., Domenech, C., Estevez, A., and Yebenes. (2003): Engineering-geological model of the Segura River flood plain (SE Spain): a Case Study for Engineering Planning. Engineering Geology, 68 (3), 171 – 187.

Douglas, B.J. and Olsen, R.S. (1981): Soil Classification Using Electric Cone Penetrometer. Symposium on Cone Penetration Testing and Experience. Proceedings of the ASCE National Convention, St. Louis, 209 – 227.

Ejasta, I. and Mangunsukarjo, K. (1990): Kajian kesesuaian lahan sawah untuk tanaman kedelai and kacang tanah melalui pendekatan unit lahan di kecamatan klungkung, Bali (*Assessment of Suitability of Paddy Fields for Soybean and Peanuts Through The Land Unit Approach in The Klungkung Sub-District, Bali*). Doctoral Dissertation, Gadjah Mada University, Yogyakarta, 105 p. (in Bahasa)

Eslami, A., Aflaki, E., and Hosseini B. (2011): Evaluating CPTu and CPTu based pile bearing capacity estimation methods using Urmiyeh Lake Causeway piling records. Scientia Iranica, 18 (5), 1009 – 1019.

Hadiwidjojo, P.M.M., Samodera, H., and Amin, T.C. (1998): Peta Geologi Lembar Bali, Nusa Tenggara (*Geological Map of Bali, Nusa Tenggara*). Scale 1: 100.000, Center for Geological Research and Development, Bandung.

Iyad, S.A, Mohammad B., Hamid N., Alireza B. (2015): Regressive approach for predicting bearing capacity of bored piles from cone penetration test data. Journal of Rock Mechanics and Geotechnical Engineering, Chinese Academy of Sciences, 7 (5), 584 – 592.

Jarushi, F., AlKaabim, S., and Consentino, P. (2015): A new correlation between SPT and CPTu for various soils. International Journal of Geological and Environmental Engineering, 9 (2), 101 – 106.

Kechebour, B.E. (2015): Relation Between Stability Of Slope And The Urban Density: Case Study. Procedia Engineering, 114, 824 – 831.

Kovacs, W.D., Salomone, L.A., and Yokel, F.Y. (1981): Energy Measurement in The Standard Penetration Test. STIN, 88 p.

Lunne, T., Powell, J.J.M, and Robertson, P.K.. (2004): Cone Penetration Testing In Geotechnical Practice. London and New York: Spon Press, London, 312 p.

Meyerhof, G.G. (1986): Penetration test and bearing capacity of cohesionless soils. Journal of Soil Mechanics and Foundations Division, 82, 1 – 19.

McCaffrey, R. and Nabalek, J. (1987): Earthquake, gravity and the origin of the Bali basin: an example of nascent continental fold-and-thrust-belt. Journal Geophysical Research: Solid Earth, 92 (B1), 441 – 460.

Volkov, N., Ivan S., and Richard J. (2017): Investigation by cone penetration tests of piled foundations in frozen soil maintained by thermosyphons. American Scientific Research Journal for Engineering, Technology, and Sciences, 31 (1), 40 – 58.

Pariseau, G.W. (2007): Design Analysis in Rock Mechanics. Taylor and Francis e-Library. University of Utah, Salt Lake City, Utah, USA, 711 p.

Rogers, J.D. (2006): Subsurface exploration using the standard penetration test and the cone penetrometer test. Environmental and Engineering Geoscience, 2, 161 – 179.

Rosye, K.R., Rutter, H.K., and Entwisle, D.C. (2009): Property attribution of 3 geological models in the Thames Gateway. London: New ways of visualizing geoscientific information. Bulletin of Engineering Geology and the Environment, 68 (1), 1.

Sanglerat, G. (1972): The Penetrometer and Soil Exploration. Elsevier Publishing Company, New York, 445 p.

Satriyo, N.A. (2017): Physical Characteristic and Bearing Capacity Analysis of Quarternary Deposit in Pendungan Coastal Area, South Bali District and Its Correlation to Facies Distribution. Master's Program Thesis, Bandung Institute of Technology, 72 p.

Schmertmann, J. (1978): Guidelines for Cone Penetration Test: Performance and Design. United State, Department of Transportation Federal Highways Administration, Report FHWA-TS-78-209.

Slatt, R.M., Jordan, D.W., D'Agostino, A.E., and Gillespie, R.H. (1992): Outcrop gamma-ray logging to improve understanding of subsurface well log correlations. Geological Society, London, Special Publications, 65 (1), 3 – 19.

SNI 4153 (2008): How to Test Field Penetration with SPT. Indonesian National Standard, National Standardization Body, 14 p.

SNI 1726 (2012): Procedure for Earthquake Resistance Planning for Building And Non-Building Structures. Indonesian National Standard, National Standardization Body, 132 p.

SNI 1727 (2013): Minimum Load For Building and Other Structure Planning. Indonesian National Standard, National Standardization Body, 196 p.

Soebowo, E., Kumoro, Y., Ruslan, M., Daryono, M.R, Sukaca, and Widodo. (2010): Model mitigasi bahaya likuifaksi untuk daerah rawan gempabumi di Daerah Sanur – Benoa, Bali Selatan (*A Liquefaction Hazard Mitigation Model for Earthquake-Prone Areas in Sanur - Benoa, South Bali*). Technical Report, Research Center for Geotechnology – LIPI, Bandung, Indonesia.

Valverde-Palacios I., Valverde-Espinosa, I., Irigaray, C., and Chacon, J. (2014): Geotechnical map of Holocene alluvial soil deposits in the metropolitan area of Granada (Spain): a GIS approach. Bulletin of Engineering Geology and Environment, 73 (1), 177 – 192.

Walker, R.G. and James, N.P. (1992): Facies Models: Response To Sea Level Change. St. John's, Nfld, Geological Association of Canada, 1 – 14 p.

URL 1: https://bali.bps.go.id/statictable/2018/04/10/47/luas-wilayah-dan-letak-geografis-pulau-bali-dan-kabupaten-kota.html (accessed on 2 February 2018)

URL 2: https://cdn.bmkg.go.id/Web/Ulasan-Guncangan-Tanah-akibat-Gempabumi-di-Selatan-Bali-1.pdf (accessed on 18 April 2018)

URL 3: https://www.pu.go.id/berita/view/15309/buku-peta-sumber-dan-bahaya-gempa-indonesia-tahun-2017.pdf (accessed on 28 July 2018)

URL 4: www.usgs.gov/products/maps/geologic-maps (accessed on 8 May 2017)

SAŽETAK

Praćenje jezgre i ispitivanje statičkim prodiranjem u analizi nosivosti kvarternoga depozita i njegova povezanost s raspodjelom facijesa na južnom Baliju

U razvoju područja važno je optimalno korištenje zemljišta i smanjenje rizika od geoloških katastrofa. Obalno područje Južnoga Balija podložno je opasnostima. Za smanjenje rizika važno je poznavati okoliš taloženja područja povezano s njegovom nosivošću i geološkim rizikom. Cilj je ovoga istraživanja ispitati podzemno taloženje i kvantificirati njegovu nosivost. Kvantitativno modeliranje provedeno je kako bi se dobio kapacitet taloženja u području Pendungan, Bali, Indonezija. Metode korištene u ovome istraživanju bile su promatranje jezgara bušotina, identifikacija uzorka krivulja ispitivanja statičkim prodiranjem (CPTu), ispitivanje svojstva indeksa sedimenata, ispitivanje čvrstoće tla i analiza nosivosti. Na temelju litološke povezanosti, uzorka krivulje CPTu-a i analize veličine zrna, u području ispitivanja izdvajaju se tri facijesa s različitim vrijednostima nosivosti. Općenito, pijesak na grebenu plaže ima veću nosivost plitkih temelja (N-SPT vrijednost od 8 do 52) od fluvijalne gline, dok poplavni facijes ima najnižu nosivost (N-SPT vrijednost 2 do 20).

Ključne riječi:
nosivost, sediment, CPTu, facijes, južni Bali

Authors' contribution

Nugroho Aji Satriyo (M.T, junior researcher, engineering geology) initialized the idea, provided bearing capacity analysis, presented the results and performed the fieldwork. **Eko Soebowo** (B.Sc, senior researcher, engineering geology) provided facies sediment analysis and performed the field work. **Imam Achmad Sadisun** (Dr. Eng, senior lecturer, geological engineering department) managed the whole process from the beginning to the end and provided statistical analysis.